Initial Stages of Interdiffusion between Asymmetrical Polymeric Layers: Glassy Polycarbonate and Melt Poly(methyl methacrylate) Interface Studied by Neutron Reflectometry

ARTICLE *in* MACROMOLECULES · DECEMBER 2013

Impact Factor: 5.8 · DOI: 10.1021/ma401895t

6 AUTHORS, INCLUDING:

Guangcui Yuan
Chinese Academy of Sciences
23 PUBLICATIONS **242** CITATIONS
SEE PROFILE

Bulent Akgun
Bogazici University
83 PUBLICATIONS **819** CITATIONS
SEE PROFILE

Macromolecules

Article

pubs.acs.org/Macromolecules

Initial Stages of Interdiffusion between Asymmetrical Polymeric Layers: Glassy Polycarbonate and Melt Poly(methyl methacrylate) Interface Studied by Neutron Reflectometry

Wenjie Du,[†,‡] Guangcui Yuan,[*,†] Mingji Wang,[†,‡] Charles C. Han,[*,†] Sushil K. Satija,[§] and Bulent Akgun[§,∥,⊥]

[†]State Key Laboratory of Polymer Physics and Chemistry, Joint Laboratory of Polymer Science and Materials, Beijing National Laboratory for Molecular Sciences, Institute of Chemistry, Chinese Academy of Sciences, Beijing 100190, China

[‡]University of Chinese Academy of Sciences, Beijing 100049, China

[§]Center for Neutron Research, National Institute of Standards and Technology, Gaithersburg, Maryland 20899, United States

[∥]Department of Materials Science and Engineering, University of Maryland, College Park, Maryland 20742, United States

[⊥]Department of Chemistry, Bogazici University, Bebek, Istanbul 34342, Turkey

ABSTRACT: Interfacial evolution of deuterated polycarbonate (dPC) and poly(methyl methacrylate) (PMMA) bilayer films supported on silicon substrates was examined by neutron reflectometry. The dPC was in the glassy state and the PMMA was in the melt state when the samples were annealed at temperatures (from 400 to 415 K) between the bulk glass transition temperature (T_g) of dPC (T_g ~ 418 K) and PMMA (T_g ~ 390 K). Asymmetric concentration profiles were observed as a result of composition dependence of the mobility. Once the slow moving dPC molecules leave the dPC-rich side (which was glassy) and enter the PMMA side, the dPC molecules become fast moving and diffuse freely in a viscous melt environment, while the fast moving PMMA molecules become slow as PMMA enter the glassy dPC matrix. Slight change in molecular mass of dPC gives rise to remarkable difference in concentration profile, indicating that mutual diffusion is very sensitive to molecular friction and entanglement of medium. With the penetration of PMMA into the dPC-rich side, the sluggish relaxation of dPC with high molecular mass results in the swelling of the dPC layer.

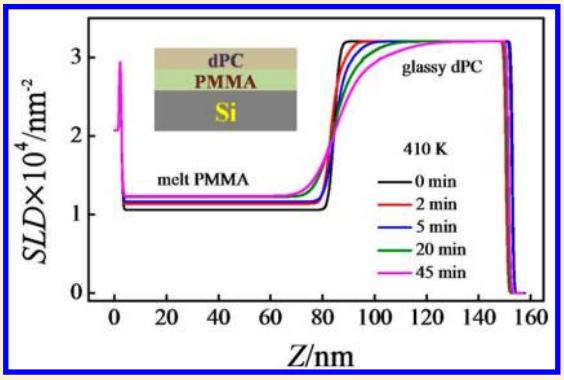

INTRODUCTION

The chain-like structure of polymer gives rise to many special effects that are unique to polymer materials science,[1] e.g., connectivity of polymer chains is one of the essential factors that determine the polymer chain dynamics. The universal features that have been shown to dominate polymer dynamics under thermal and compositional equilibrium are Rouse motion,[2] entanglement,[3,4] and reptation.[5,6] The Rouse model is the foundation on which the most current and more sophisticated interpretations of polymer dynamics, including interdiffusion, are built upon. The basic assumption in the Rouse model is that each bead in the macromolecule feels the same friction and the macromolecule feels the cumulative effect.[2] The dynamic mean-field notion of a single average friction coefficient for a polymer chain is acceptable in chemically identical media. However, this assumption is probably inapplicable in polymer interdiffusion which by definition refers to diffusion across boundaries, surfaces, interfaces and in gradients, because the thermodynamic interactions and the friction experienced by an individual polymer segment (or "bead") may depend on the time and environment as the interdiffusion process is proceeding. Therefore, in this study of interdiffusion we focus our attention on how specific molecules behave and interact with the local environment, and the most fundamental question to ask is the molecular level understanding of segmental friction coefficients in polymer mixtures.[1]

Some theoretical and experimental efforts on understanding the segmental dynamics in miscible polymer mixtures have been put forward recently.[7−11] Lodge and Mcleish[7] have proposed a model to describe the composition and temperature dependence of monomeric friction factor in polymer mixtures by emphasizing the importance of "self-concentration", the local enrichment in like monomers which is an inevitable consequence of chain connectivity. The Lodge−Mcleish model has been shown to be able to provide a nearly quantitative description of monomeric friction factor at temperatures sufficiently far above the glass transition temperature (T_g) in several cases,[12−14] and it is able to account for many of the observed phenomena in a qualitative manner.[15] For example,

Received: September 12, 2013
Revised: December 2, 2013
Published: January 7, 2014

   dx.doi.org/10.1021/ma401895t | Macromolecules 2014, 47, 713−720

this model accounts for the observation that the faster component with lower T_g tends to have segmental dynamics in the blend closer to its own bulk, whereas the slower component with higher T_g senses a blend average.[7] Meanwhile, the thermal concentration fluctuation has not been taken into account in the Lodge−Mcleish model.

One of the key ideas of previous theories on polymer interdiffusion, such as the slow mode theory which was originally calculated by Brochard et al.[16] and Binder[17] and the fast mode theory which was proposed by Kramer et al.[18] and Sillescu,[19] is to express the interdiffusion coefficient of a polymer mixture as a product of thermodynamic and kinetic factors. As remarks on these noninteracting cases, the thermodynamic factor only depends on the static correlation function of composition fluctuation, and the kinetic factor involves friction coefficient which characterizes the diffusion of the two types of polymer chains but does not depend on the effective interactions.[20,21] These theories are all based on the assumption that the mobility of an individual polymer chain is essentially only molecular weight dependent. In other words, the fast molecules are always fast and the slow ones are always slow even when they move across the interface and into another matrix. Of course, real mixtures are always to some extend interacting, so theories on polymer−polymer interdiffusion should take into account intra- and intermolecular friction which may depend on the volume fractions and on temperatures.[21] It should be pointed out that both the fast mode and slow mode models mentioned above are addressing the concentration fluctuation (or relaxation) around an average concentration. Therefore, any experiment that is designed to test the models by using chemically dissimilar couples has to be carried out in a concentration condition such that either the concentration gradient or the concentration difference between the two testing layers approaches zero.[22−24] In these experiments,[23,24] because of the small jump in composition at the interface, the mutual diffusion can be assumed to be governed by a single mutual diffusion coefficient which corresponding to the average composition of such a couple, and classical error functions are normally used for the concentration profiles across the interfaces.

Many practical and useful applications, such as welding, coating, adhesion, and friction, are concerned with the interdiffusion between two chemically different pure polymers.[25] In these cases, the mutual diffusion coefficient varies with the spatial distribution of concentration because the thermodynamic interactions are concentration dependent as given by Flory−Huggins theory,[6] and the frictional interactions are also concentration dependent as described in the framework of Haley and Lodge.[15] The distances between the measurement temperature and the component T_gs, and between the components viscosities, are important parameters controlling the composition dependence of linear viscoelastic properties of polymer mixtures which are germane to interdiffusion. For interfacial mixing of a polymer pair where both components are relatively mobile, interdiffusion is Fickian-like but with a concentration-dependent diffusion coefficient, and error functions are used for concentration profiles across the interfaces.[26] For interfacial mixing of a polymer pair with large mismatch in their respective molecular mobilities, such as the cases for which one of the components is a glass and the other is in melt state, strong variations in mutual diffusion coefficient with concentration give rise to a strongly distorted profile.[27−30] In all but very few prior studies of interdiffusion of a melt polymer across a glassy polymer interface, there are large T_g differences between the two components, e.g., 135 K between polystyrene (PS) and poly(vinyl methyl ether) (PVME) in Sauer and Walsh's work,[29] 110 K between poly(xylenyl ether) (PXE) and PS in Composto and Kramer's work,[30] 130 K between poly(2,6-dimethyl-1,4-phenylene oxide) (PPO) and PS in Lin et al.'s work,[27] 120 K between lithium salt of a lightly sulfonated polystyrene ionomer (Li-SPS) and poly(*N*,*N*′-dimethylethylenesebacamide) (mPA) in Weiss et al.'s work.[28] Although the detailed diffusion kinetics in polymer couples mentioned above are different, an asymmetric interfacial concentration profile and a sharp front moving toward the glassy side, like diffusion process of solvent molecules into glassy polymer, were observed.

In the present work, we examine the interfacial evolution of a deuterated polycarbonate/poly(methyl methacrylate) (dPC/PMMA) bilayer by annealing at temperatures (from 400 to 415 K) between the bulk T_g of dPC ($T_g \sim 418$ K) and PMMA ($T_g \sim 390$ K). The issue of PC/PMMA blend miscibility has been extensively investigated by many independent polymer research groups,[31−38] but the seemingly simple issue of what is the coexistence curve of PC/PMMA blend has been a long-argued problem.[37] Kyu and co-workers[33,34] indicated that the PC/PMMA blend had a lower critical solution temperature (LCST) located well above its corresponding T_gs. Yet, long time annealing experiments by Paul and co-workers[36] claimed that PC/PMMA blend may have only a very narrow (or no) miscible region above its T_g line. The discrepancy is partially due to the so-called solvent effect[31,32] and partially due to the crossing or interference of T_g with the coexistence temperature of finite composition for sample preparation and physical measurement. Motowoka and co-workers[37] showed that the phase diagram of the dPC/PMMA blend ($M_w = 2.8 \times 10^4$ g/mol for dPC and $M_w = 3.3 \times 10^4$ g/mol for PMMA), even though it is buried below its T_g, is possible to precisely obtain by studying the kinetics of early stage phase separation near and above its T_g with time-resolved small-angle neutron scattering. In the present paper, we investigated the reverse process of phase separation—the interdiffusion of two pure components across the interface, and only the initial stage of interdiffusion was concerned. In this initial stage of interdiffusion, in the PMMA-rich side, local composition is still staying in the miscible gap, and the experimental temperature is higher than the local T_g. Molecular mass effects were also investigated since they reveal the physical nature of the interface broadening process. Given that the monomeric friction factor can vary several orders of magnitude over relatively modest temperature intervals above T_g in simple homopolymers, we will address a central issue of broad technological and scientific interest: how do glass transition (specifically molecular friction) and entanglement sensitively affect the evolution of polymer interfaces brought into contact? The observations of the present study on interdiffusion between polymer films are contrasted with prior observations which have been made at temperatures much higher than the T_gs of both components, and which at temperatures between T_gs of both components but with a large discrepancy between the measurement temperature and the component T_gs.

EXPERIMENTAL SECTION

Sample Preparation. Deuterated bisphenol A polycarbonate was synthesized following a procedure reported by Yoon et al.[39] with phenol and acetone-d_6 as starting materials. Bisphenol-A-d_6 used for

dx.doi.org/10.1021/ma401895t | *Macromolecules* 2014, 47, 713−720

the polycondensation reaction was washed with water and dried before recrystallized three times from toluene. The final product dPC was purified by dissolving in chloroform and precipitating into methanol. Then the polymer was filtered and washed with 348 K hot water. The purification procedure was repeated three times. Two dPC samples with different molecular mass were used in this study and represented by dPC-L and dPC-H as shown in the following analysis. The number-average molecular mass and the polydispersity determined by gel permeation chromatography (GPC) (comparing with polystyrene standard) with *N*,*N*-dimethylformamide (DMF) as the solvent were 4.3×10^4 g/mol and 1.53 for dPC-L and 6.8×10^4 g/mol and 2.3 for dPC-H. The GPC profiles of the two dPC samples are shown in Figure 1. The PMMA used for this study was purchased from Acros

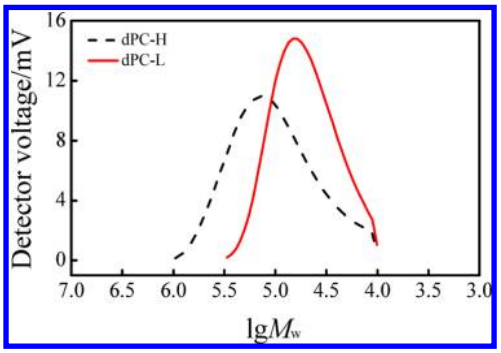

Figure 1. GPC profiles of dPC-H ($M_n = 6.8 \times 10^4$ g/mol, $M_w = 1.6 \times 10^5$ g/mol, $M_w/M_n = 2.3$) and dPC-L ($M_n = 4.3 \times 10^4$ g/mol, $M_w = 6.6 \times 10^4$ g/mol, $M_w/M_n = 1.53$) with DMF as the solvent.

Organics,[45] and its number-average molecular mass and the polydispersity determined by GPC (comparing with polystyrene standard) with DMF as the solvent were 3.8×10^4 g/mol and 1.52, respectively.

The glass transition temperature of dPC and PMMA used in this study are 418 and 390 K as measured by differential scanning calorimetry (Mettle Toledo DSC822e)[54] with a heating rate of 10 K/min for the second heating cycle. The DSC traces of pure dPC and PMMA components are shown in Figure 2. The onset and the

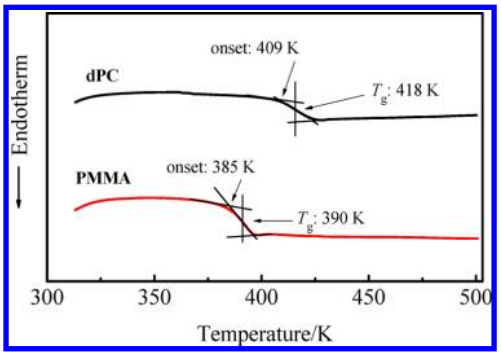

Figure 2. DSC traces of pure dPC-L and PMMA components with a heating rate of 10 K/min.

midpoint of the heat capacity change during the glass transition are indicated. The T_g is determined as the midpoint temperature. Although the size distributions of the low molecular weight tails of these two dPC materials are different, there is no detectable difference in the onset of the heat capacity change during DSC measurement of two dPC samples. This is probably due to the very small average molecular weight between entanglement points (M_e) in bisphenol A polycarbonate which was determined as 1660 (equivalent to 6.5 repeating units).[48] The relevant molecular weight, which is the critical for T_g (M_c), is twice M_e. The average molecular weights of both dPC samples are much larger than M_c of dPC. Thus, the amount of small dPC molecules with molecular weight lower than M_e, which can significantly decrease the T_g, was quite low.

The samples prepared for the neutron reflectivity (NR) experiment are dPC/PMMA bilayer films consisting of a dPC layer on top of a PMMA layer with polished silicon wafers as substrates (7.5 cm diameter, 0.5 cm thickness). The bilayer samples were prepared by spin-coating and floating techniques. Prior to spin-coating, the silicon wafers were cleaned in an acid bath of H_2SO_4/H_2O_2 (3/1) mixture for 45 min at 353 K, followed by thoroughly rinsing in deionized water. The PMMA layer was prepared from a 25 mg/mL PMMA solution in toluene which was first filtered through a 0.2 μm PTFE filter and then spun-cast onto the clean silicon wafer. After spin-coating, the PMMA film was first air-dried and then dried in a vacuum oven for 1 h at 423 K. The top dPC layer was prepared by spin-coating a solution of dPC in 1,1,2,2- tetrachloroethane on another clean silicon wafer. By immersing the wafer into distilled water, the dPC layer was floated off onto the water surface and then picked up on the wafer which has been spin-coated with PMMA in advance. Ellipsometry (M-2000VI, J.A. Woollam Co., Inc.)[54] was used to characterize the single films with respect to film thickness and surface roughness. Residual solvent can be a problem in cast polymer films so the bilayer films were placed under vacuum at 343 K for 48 h to remove residual solvent and water trapped between the layers before use. The thickness of the single dPC film is about 75 or 45 nm, and the thickness of the single PMMA film is about 80 nm.

Interdiffusion was accomplished by inserting the bilayer sample in a large slotted aluminum block, preheated to desired temperatures in vacuum oven. The sample was centered inside the heating aluminum block enclosure with a small gap; thereby the transfer of heat to the sample was maximized mainly through conduction. Hence, the time required for the sample to reach the desired temperature for the interdiffusion experiment was of no significant consequence. The sample temperature while in the oven was monitored by a thermometer inserted into the heating block. The temperature was controlled to ±0.3 K. After a desired interdiffusion time, the specimens were quenched to room temperature by placing the substrate on a cool metal block. The time required to cool the specimen to temperature below the T_g of PMMA (390 K), which will halt the interdiffusion process, was less than 20 s. All reflectivity experiments were performed at room temperature.

Reflectivity Measurement. The NR measurements were performed at the National Institute of Standards and Technology Center for Neutron Research (NCNR) using a NG-7 horizontal reflectometer. The wavelength (λ) of the neutron used is 0.475 nm with $\Delta\lambda/\lambda$ around 0.02. The reflectivity measurements were performed over a range of angles, and the data were presented as a function of the neutron momentum transfer perpendicular to the surface, $q = (4\pi/\lambda) \sin\theta$, where θ is the incident angle of the neutron radiation. The angular divergence of the beam was varied through the reflectivity scan, and this provided a relative q resolution $\Delta q/q$ of 0.025. Since reflectivity observations are sensitive to the in-plane averaged neutron scattering length density (SLD) profile perpendicular to the sample surface, the SLD values are used to determine concentration profiles. The SLD values for dPC, PMMA, silicon oxide, and bulk silicon are 3.20×10^{-4}, 1.06×10^{-4}, 3.48×10^{-4}, and 2.07×10^{-4} nm^{-2}, respectively. Programs from the Reflpak Suite were utilized for our data reduction and analysis.[40]

RESULTS AND DISCUSSION

Asymmetric Interfacial Profile in the Glassy/Melt Interface. A typical set of neutron reflectivity profiles at different annealing times are displayed in Figure 3, with each respective profile offset log $R = 2$ for clarity. The symbols are the experimental data, and the solid lines are the theoretical fits to the data from model density profiles which are shown in Figure 5b. The initially prepared bilayer sample has a reflectivity profile with distinct interference fringes with a spacing determined by the thickness of the deuterated PC layer. As

dx.doi.org/10.1021/ma401895t | *Macromolecules* 2014, 47, 713−720

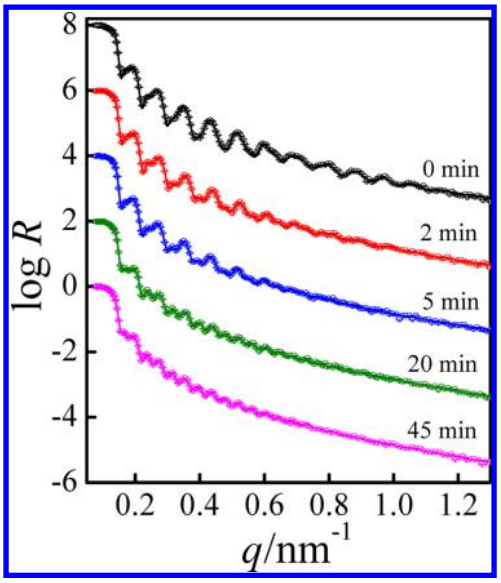

Figure 3. Neutron reflectivity spectra for dPC-L/PMMA bilayer sample on a silicon substrate annealed at 410 K for different times.

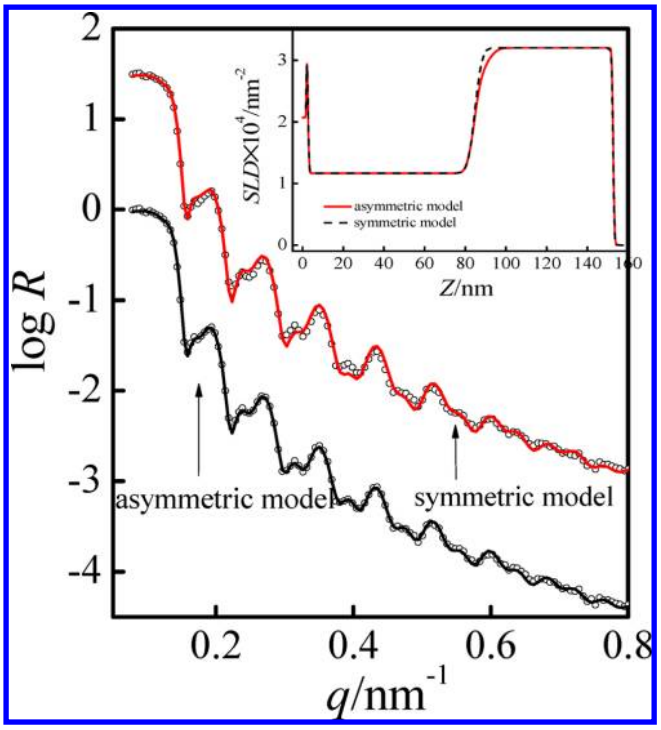

Figure 4. Neutron reflectivity profiles from dPC-L/PMMA bilayer samples on silicon substrates annealed at 410 K for 5 min. The inset gives the profiles of scattering length density as a function of layer depth (Z) from symmetric model and asymmetric model. The symbols represent the NR data, and the solid line represents the reflectivity calculated by using the inset SLD profile.

the sample was annealed at 410 K, which is between the T_gs of the two components, the fringes at higher q values gradually being damped out showed that the interface between the layers began to broaden. The modulation periods did not shift after annealing so that the thermal treatment did not change the layer thickness. Additionally, higher order oscillations became visible which was arising from reflections from the overall thickness of the bilayer sample. Finally, with further broadening of the interface between the two polymer layers, the form of the reflectivity curve was significantly influenced by the air/dPC and the PMMA/silicon interfaces.

In general, error functions are used to fit interfacial profiles, including those between air/dPC and PMMA/silicon interfaces. While the profile for the sample as made can be successfully fitted by assuming a diffuse Gaussian roughness at the dPC/PMMA interface, this model is very unsatisfactory for the annealed samples. It is necessary to change the model for the SLD profile at the interface of annealed samples because of a large mismatch in the molecular mobility of the polymers on either side of the interface. Here, when the annealing temperatures (e.g., 410 K) are above the T_g of PMMA but below the T_g of dPC, one may expect that the penetration of PMMA chains into the glassy dPC-L will be much slower than the penetration of dPC chains into the viscous melt PMMA layer. As a result, an asymmetric interfacial composition profile is probably more realistic. The requirement of an asymmetric model has been also noted in studies of interdiffusion between partially miscible polymers,[41,42] interdiffusion between glassy/melt interface,[28] interdiffusion near an attractive solid substrate,[43,44] and interdiffusion at short times.[45,46] The distorted profiles are all resulted from the asymmetrical effect of medium on the dynamics experienced by an individual polymer. In all cases, the sum of two Gaussian functions is sufficient to yield a suitable fit to the data. For instance, in Figure 4, the reflectivity of a dPC-L/PMMA sample after annealing at 410 K for 5 min is partially shown, and the least-squares fits of reflectivity data by the symmetric and asymmetric model are compared. For the symmetrical model using only one single Gaussian function with a characteristic parameter of root-mean-square variance, σ = 6.6 nm, the fits agree well with the data only for $q > 0.5$ nm^{-1}. This suggests that two widths with one small and one large are needed to accommodate the observed reflectivity data. The asymmetric model combining two Gaussian functions with different values of the characteristic width (σ_1 = 8.5 nm, σ_2 = 6.5 nm) on each side of the interface is more successful at representing the interference fringe features at the whole q range. The asymmetric model especially captures small-amplitude oscillations better than the symmetric model does. The σ_1 represents the interfacial width toward the dPC layer and is larger than σ_2, which characterizes the interfacial width toward the PMMA layer. The subtle differences between two real space profiles demonstrate the sensitivity of the reflectivity technique to the functional form of the SLD profile. Subsequently, the asymmetric model fits were used on all the spectra of annealed samples measured in this study. However, it should be noted that while the asymmetric model is an improvement over the symmetric model, it is not necessarily the best model or the most accurate representation of the interfacial composition profile. The asymmetric model is significant only within the resolution of these experiments; it suitably represents the general features of the composition profile of the interface.[28]

Temperature Effect on the Diffusion Process. The obtained temporal evolutions of interfacial SLD profiles at different annealing temperatures are presented in Figure 5. The SLD profile in Figure 5b was the one used to generate the reflectivity fits (solid lines) in Figure 3. The data in Figure 5 yield the following three observations regarding the interfacial mixing in this system: (1) Initially prepared films have very sharp interfaces between the dPC and the PMMA layers with interfacial width about 3.0 nm. The asymmetry of the interfacial

dx.doi.org/10.1021/ma401895t | Macromolecules 2014, 47, 713−720

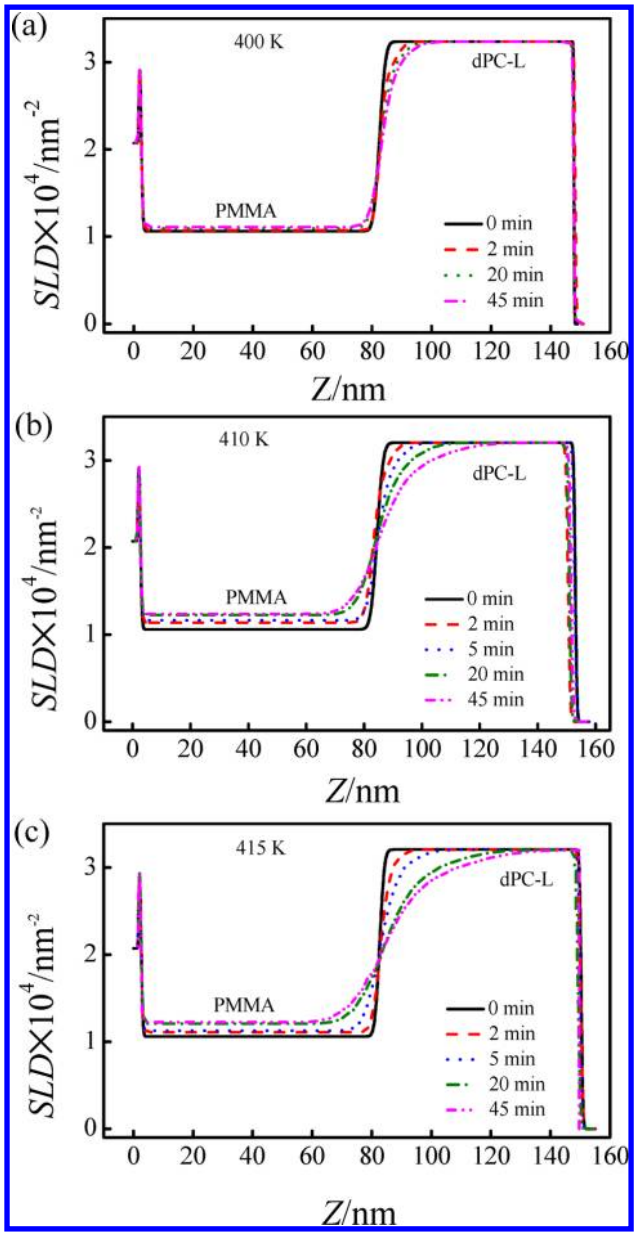

Figure 5. Evolution of the scattering length density profile at different annealing temperatures at different times for the dPC-L/PMMA bilayer sample on silicon: (a) 400, (b) 410, and (c) 415 K. The thickness of PMMA layer is about 80 nm, and the thickness of dPC layer is about 75 nm.

SLD profiles are clearly seen when the samples were annealed. The SLD profiles generally have a steep central part corresponding to the initially sharp interface with broader concentration gradients on the dPC-rich side. (2) With the increasing of annealing time and temperature, one finds an increase of width σ_1 and σ_2 and a decrease in the step height. (3) The glassy dPC layer is gradually softened by the viscous melt PMMA, but dPC concentration in the PMMA layer is approximately constant. The fact that dPC concentration in the PMMA side is approximately constant and increases with time indicates that once the slow moving dPC molecules leave the dPC-rich side (which is glassy) and enter the PMMA side (which is melt), the dPC molecules will become fast moving in a viscous melt environment and diffuse quickly to the bulk of PMMA; finally, the dPC molecules ejected from the interface disperse themselves within the PMMA bulk fairly uniformly. Here, the fits are performed under the constraint that the mass of each component is conserved to within 5%. It should be emphasized that the analysis of these reflectivity data is only sensitive to the thickness of the deuterated layer and the concentration profile of the polymer−polymer interface. A small layer with a slightly higher SLD on PMMA side of the interface was introduced while fitting to check the possibility of large gradients or localized enrichment of dPC in the PMMA layer. Nevertheless, the distribution of dPC in the PMMA-rich side which is not localized but is homogeneously distributed or which may have a very small concentration gradient but is averaged as homogeneous within the resolution of NR could due to the fact that dPC become fast moving in a viscous melt environment.

Since the molecular weight of dPC materials is not monodisperse, a question followed naturally is about the role of low molecular weight species in dPC layer. If the rapid movement of the dPC leading edge on the PMMA-rich side is mainly associated with the low molecular weight tails in the size distribution of dPC material, which is movable and miscible in PMMA region under given temperature, the movement will stop when the supply of mobile species is exhausted. Figure 6

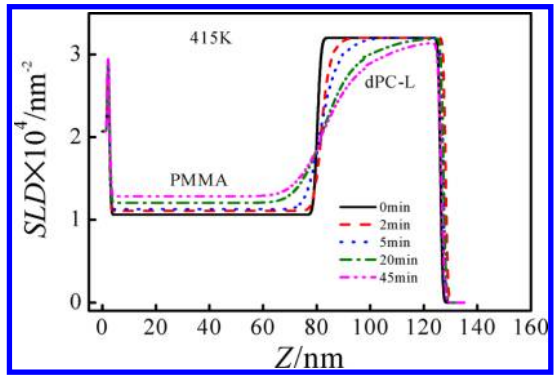

Figure 6. Evolution of the scattering length density profile for a dPC-L/PMMA bilayer sample on silicon annealed at 415 K for different times. The thickness of PMMA layer is 80 nm, and the thickness of dPC-L layer is 45 nm.

shows the evolution of the interfacial SLD profile from a bilayer sample with thin dPC-L layer on top (45 nm). As compared to bilayer film with thick dPC layer on top in Figure 5c, a continuous interdiffusion across the interface is also observed for thin bilayer film annealed at 415 K for 45 min. The amount of dPC ejected into the PMMA-rich size has no significant difference for both samples. The miscible dPC component in the PMMA-rich side could be estimated from the increasing of the integral area under the SLD profile in the PMMA-rich side. After the bilayer films were annealed at 415 K for 45 min, there was about 10% of dPC in thick sample (Figure 5c) and about 20% of dPC in thin sample (Figure 6) move across the glassy/melt interface, respectively. These ratios are quite large compared with the tails of molecular weight distribution, although it is hard (or impossible) to tell what the fraction is for chains that should be mobile and what the fraction is for chains that should be frozen from the size distribution of dPC for a given annealing temperature in the glass transition region. It could be told that, in this stage of interdiffusion, in the PMMA-rich side, local composition is still staying in the miscible gap and the experimental temperature is higher than the local T_g.

dx.doi.org/10.1021/ma401895t | Macromolecules 2014, 47, 713−720

Considering the dynamic properties of miscible polymer blends, it is often the case that the faster component shows dynamics more reminiscent of its melt, whereas the slow component will be closer to the average dynamics of the blend. This phenomenon has been the subject of numerous studies.[15] The Lodge−Mcleish model, which places particular emphasis on self-concentration with a length scale of Kuhn length, provides a quantitative explanation of this phenomenon successfully.[7,13,47] Here, our observations of interdiffusion between a glassy/melt interface with large concentration gradient can be qualitatively explained in the framework of the Lodge−Mcleish model[7] although it describes the blend dynamics at temperature sufficiently far above T_g. According to the Lodge−Mcleish model,[7] the larger the self-concentration, the more the average dynamics of that component in the mixture will resemble the dynamics in the pure component. Here, PMMA is the flexible component and will have the larger self-concentration. Therefore, it is reasonable that the dPC molecules ejected from the interface quickly and dispersed themselves within the PMMA bulk uniformly. From the above observations, we can conclude that the medium with different molecular friction coefficients will affect the mobility of foreign molecules. That is, the slow one becomes fast as dPC goes into PMMA and the fast one becomes slow as PMMA enters the glassy dPC region in our system. Therefore, for interfacial mixing between two pure polymers in which one component is a melt and the other is a glass, a markedly asymmetric concentration versus depth profile is expected as a result of composition dependent on mobility. A quick dispersion of ejected slow component in the fast matrix has also been observed in other glassy/melt polymer interface, e.g., PXE/PS interface,[30] PPO/PS interface,[27] and Li-SPS/mPA interface.[28] The concentration profiles in those previously reported systems are qualitatively similar to what is reported herein for the dPC/PMMA system on the fast-component-rich side, but there are differences on the slow-component-rich side which will be discussed in the next section. Therefore, the free moving of slow component in fast matrix is not unique to our system. Furthermore, in the above-mentioned works,[27,28,30] the slow component is either polydisperse (PXE: M_w/M_n = 2.3; PPO: M_w/M_n = 3.0) or monodisperse (Li-SPS: M_w/M_n = 1.07), and the phenomenon of rapid diffusion of slow component in fast matrix was observed not only in initial stage but also after long time of interdiffusion. Since this phenomenon is not confined by the initial stage interdiffusion and the dispersity, the low molecular weight species might not have a dominant effect on the rapid diffusion.

Molecular Weight Effect on the Diffusion Process. The SLD profiles of a dPC-H/PMMA bilayer film annealed at 415 K are shown in Figure 7 and are compared with that of the dPC-L/PMMA bilayer film annealed at the same temperature (Figure 5c). It can be seen that in the dPC-H/PMMA bilayer a remarkably swollen front moves toward PMMA side, and a steep step remains during annealing. It is assumed that tracer diffusion coefficient of PMMA chain inside the dPC layer is the same for both cases because of the same molecular friction coefficient, but the release of dPC chain with high molecular weight is more sluggish than shorter chain due to the entanglement constraints. The M_e for PC is 1660, which is equivalent to 6.5 repeating units and abnormally small as compared to PMMA (12 500) and PS (16 600).[48] For entangled polymers, according to the reptation model proposed by de Gennes,[6] the longest relaxation time (τ_{rep}) for an entire

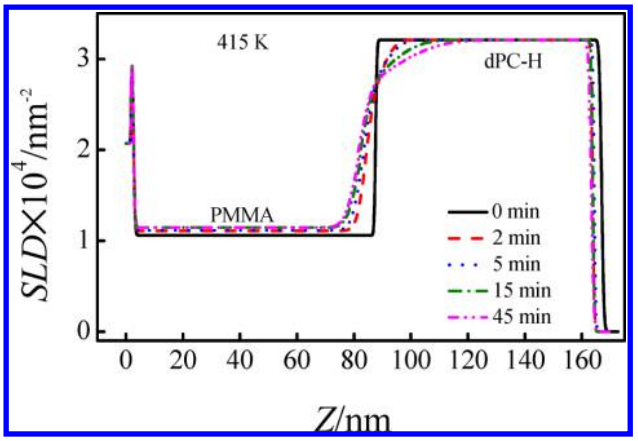

Figure 7. Evolution of the scattering length density verse depth profile for a dPC-H/PMMA bilayer sample on silicon annealed at 415 K for different times.

chain to renew its configuration is to the third power of the molecular weight dependent, $\tau_{rep} \sim M^3$. The number-average molecular weights of the two test samples are 4.3×10^4 g/mol for dPC-L and 6.8×10^4 g/mol for dPC-H. The difference in the molecular weight is quite limited and may not result to detectable difference at high temperature relaxation behavior (above T_g, the time scale could be in seconds). However, according to the time−temperature correspondence principle, for the slow relaxation behavior at low temperature (close to T_g, the time scale could be in hours), the distinction resulted from the difference in the molecular weight may be magnified to become significant. Thus, when the same amount of PMMA chains goes into the dPC layer as driven by the excess enthalpy and entropy of segment mixing, less dPC-H chains are extruded out of the interface, resulting in the swelling of dPC layer.

The observation in Figure 7 that the interfacial front moves toward the viscous melt PMMA side during annealing is not in agreement with the prior investigation in other glassy/melt polymer systems,[27−30] in which the interfaces were all found to move toward the glassy side. We believe that this phenomenon is mainly related to the discrepancy between the measurement temperature and the component T_gs. The T_g differences between dPC and PMMA is about 28 K, which is much smaller than the large T_g discrepancy in other reported glassy/melt polymer couples, e.g., 135 K between PS and PVME in Sauer and Walsh's work,[29] 110 K between PXE and PS in Composto and Kramer's work,[30] 130 K between PPO and PS in Yang et al.'s work,[27] and 120 K between Li-SPS and mPA in Weiss et al.'s work.[28] The process that a more mobile component diffuses into a glassy component can be treated as a visco-plastics extrusion process which can be explained by the mechanistic model of case II diffusion of Argon et al.[49] When the bilayer sample is annealed at a temperature that is between the T_g of two pure components, with the diluent (component with low T_g) penetrating into the glassy solid, the T_g of the diluent-laden glassy material will gradually decrease and finally may be below the annealing temperature. For the polymer couple with large T_g discrepancy, when the annealing temperature is far below the T_g of the slow component, the role of the component with low T_g is like small molecules in typical case II diffusion, which generally describes the diffusion process of solvent molecules into glassy polymer and is characterized by a sharp front moving into the glassy polymer with a constant velocity. However, for our current system of the

dPC/PMMA couple with a small T_g difference, the concentration profile is more sensitive to annealing temperature and molecular weight of the slow component because a small change in composition of the diluent-laden material in the interfacial zone will determine whether the slow chain is to be ejected into the fast viscous melt matrix or stay in the entangled and/or glassy state. Higher volume fraction of dPC-H in the diluent-laden zone is probably due to the slow relaxation of highly entangled dPC-H chains even after the gradually swelling by the lower T_g component, and this yields a steeper composition gradient.

The range of uncertainty in each fitted parameter was determined by fixing that parameter at various values and allowing the other parameters to vary in the fitting within physically reasonable limits, and in this way the maximum uncertainty of the fitted parameters in comparison to the data was found to be about 5%. The primary parameter extracted from the fits to the reflectivity data is the interfacial width in the glassy dPC side (σ_1). The initial roughness on dPC side σ_0 which is calculated as the half of interfacial width between the bilayers before annealing is quadratically subtracted through the function of $\Delta\sigma_1 = (\sigma_1^2 - \sigma_0^2)^{1/2}$. The value of $\Delta\sigma_1$ can be taken as a measure of the interfacial broadening during thermal annealing. Figure 8 plots $\Delta\sigma_1$ as a function of annealing time

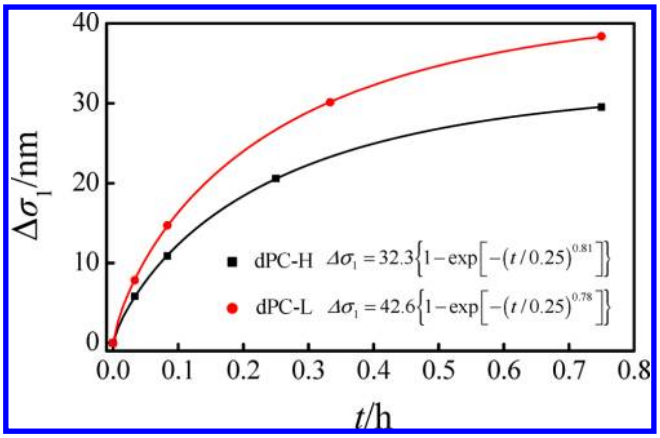

Figure 8. Interface front movement on dPC side as a function of annealing time (t) at 415 K for dPC/PMMA bilayer samples. The thickness of PMMA layer is 80 nm and the thickness of dPC layer is 75 nm. The solid lines represent the fitting results from a stretched exponential function as shown in eq 1.

for dPC-L/PMMA and dPC-H/PMMA bilayer samples annealed at 415 K. It can be seen that $\Delta\sigma_1$ increases with annealing time first quickly and then slowly. We describe this kinetics by a stretched-exponential function[50−52]

$$\Delta\sigma_1 = \sigma_\infty\{1 - \exp[-(t/\tau)^\alpha]\} \quad (1)$$

where σ_∞ describes the long time ($t \to \infty$) "plateau value" of $\Delta\sigma_1$ and τ denotes the characteristic evolution time. This simple model provides a good description of our data. The solid lines, which represent best fits to the experimental data, are shown in Figure 8. The fitting parameters for dPC-H/PMMA were $\Delta\sigma_\infty = 32.3 \pm 0.2$ nm, $\tau = 0.25 \pm 0.01$ h, and $\alpha = 0.81 \pm 0.01$, and those for dPC-L/PMMA sample were $\Delta\sigma_\infty = 42.6 \pm 0.4$ nm, $\tau = 0.25 \pm 0.01$ h, and $\alpha = 0.78 \pm 0.01$. The apparent interfacial broadening (a combination of that in PMMA side and that in dPC side) during thermal annealing depends on the rate of the whole chains moving in the PMMA-rich side when the chains are completely released and the rate of chain segment relaxation when part of the chains is still frozen in the glassy dPC-rich side. As we describe the apparent interfacial broadening in the PMMA-rich side and that in the dPC-rich side separately in this study by an asymmetrical fit combining two Gaussian functions with different values of the characteristic width on each side of the interface, it is reasonable that the broadening of the profile on the dPC side is on the order of R_g and depends on molecular weight of dPC. However, the characteristic evolution time τ, which describes the relaxation (softening) rate of dPC chain segment with respect to the annealing temperature, is molecular weight independent for highly entangled polymer. Similar arguments about the application of eq 1 have been made for surface-limited diffusion in polymer adsorption and desorption from solution,[52] for compatibilization of polymer blends by complexation,[28] for diffusion in glassy state,[50] and for hole growth in thin block copolymer films.[53] The arguments imply that the stretched-exponential kinetics could describe a general class of physical process that are rate limited by diffusion at a surface of component with low mobility.

CONCLUSIONS

Neutron reflectometry was used to study the initial stage of interdiffusion between glassy dPC and viscous melt PMMA interface. The interfacial profiles between two polymer layers were systematically investigated as a function of time, molecular mass, and for a range of annealing temperatures (400−415 K) between the bulk glass transition temperatures of the two components. The annealing temperatures are very close to the component T_gs. It was found that the remarkable asymmetric profile resulted from concentration dependent mobility is very sensitive with the annealing temperature and molecular mass. Once the slow-moving dPC molecules left the dPC-rich side (which is glassy) and entered the PMMA side, dPC molecules became fast moving in a viscous melt environment and diffused quickly within the bulk of PMMA. With the penetration of PMMA to the dPC-rich side, sluggish relaxation of dPC with high molecular mass resulted in the swelling of dPC layer. The kinetics of diffusion toward the slow-moving dPC side can be described by a stretched-exponential function, which may describe a general class of physical processes that are rate limited by diffusion of component with low mobility at a surface or interface. In scientific research of interdiffusion, more data of higher precision are needed in order to draw better and universal conclusions, especially about the very early stage of interpenetration, about molecular weight dependence, and about the different stages of the diffusion processes.

AUTHOR INFORMATION

Corresponding Authors

*Ph +86 10 82618089; Fax +86 10 62521519; e-mail gcyuan@iccas.ac.cn (G.Y.).

*Ph +86 10 82618089; Fax +86 10 62521519; e-mail c.c.han@iccas.ac.cn (C.C.H.).

Notes

The authors declare no competing financial interest.

ACKNOWLEDGMENTS

This work is supported by the National Basic Research Program of China (973 Program, 2012CB821500) and the Chinese National Science Foundation (Project 21004069).

REFERENCES

(1) Kausch, H. H.; Tirrell, M. *Annu. Rev. Mater. Sci.* **1989**, *19*, 341.
(2) Rouse, P. E. *J. Chem. Phys.* **1953**, *21*, 1272.
(3) Edwards, S. F. *Proc. Phys. Soc., London* **1967**, *92*, 9.
(4) Aharoni, S. M. *Macromolecules* **1983**, *16*, 1722.
(5) Doi, M.; Edwards, S. F. *The Theory of Polymer Dynamics*; Clarendon Press: Oxford, 1986.
(6) de Gennes, P. G. *Scaling Concepts in Polymer Physics*; Cornell University Press: Ithaca, NY, 1979.
(7) Lodge, T. P.; McLeish, T. C. B. *Macromolecules* **2000**, *33*, 5278.
(8) Adams, S.; Adolf, D. B. *Macromolecules* **1999**, *32*, 3136.
(9) Kumar, S. K.; Colby, R. H.; Anastasiadis, S. H.; Fytas, G. *J. Chem. Phys.* **1996**, *105*, 3777.
(10) Zetsche, A.; Fischer, E. W. *Acta Polym.* **1994**, *45*, 168.
(11) Roland, C. M.; Ngai, K. L. *J. Rheol.* **1992**, *36*, 1691.
(12) Leroy, E.; Alegria, A.; Colmenero, J. *Macromolecules* **2002**, *35*, 5587.
(13) Haley, J. C.; Lodge, T. P.; He, Y. Y.; Ediger, M. D.; von Meerwall, E. D.; Mijovic, J. *Macromolecules* **2003**, *36*, 6142.
(14) He, Y. Y.; Lutz, T. R.; Ediger, M. D. *J. Chem. Phys.* **2003**, *119*, 9956.
(15) Haley, J. C.; Lodge, T. P. *J. Rheol.* **2004**, *48*, 463.
(16) Brochard, F.; Jouffroy, J.; Levinson, P. *Macromolecules* **1983**, *16*, 1638.
(17) Binder, K. *J. Chem. Phys.* **1983**, *79*, 6387.
(18) Kramer, E. J.; Green, P.; Palmstrom, C. J. *Polymer* **1984**, *25*, 473.
(19) Sillescu, H. *Makromol. Chem., Rapid Commun.* **1984**, *5*, 519.
(20) Akcasu, A. Z.; Nagele, G.; Klein, R. *Macromolecules* **1995**, *28*, 6680.
(21) Jilge, W.; Carmesin, I.; Kremer, K.; Binder, K. *Macromolecules* **1990**, *23*, 5001.
(22) Feng, Y.; Han, C. C.; Takenaka, M.; Hashimoto, T. *Polymer* **1992**, *33*, 2729.
(23) Composto, R. J.; Kramer, E. J.; White, D. M. *Macromolecules* **1992**, *25*, 4167.
(24) Composto, R. J.; Kramer, E. J.; White, D. M. *Nature* **1987**, *328*, 234.
(25) Yuan, B. L.; Wool, R. P. *Polym. Eng. Sci.* **1990**, *30*, 1454.
(26) Schubert, D. W.; Stamm, M.; Muller, A. H. E. *Polym. Eng. Sci.* **1999**, *39*, 1501.
(27) Lin, H. C.; Tsai, I. F.; Yang, A. C. M.; Hsu, M. S.; Ling, Y. C. *Macromolecules* **2003**, *36*, 2464.
(28) Feng, Y.; Weiss, R. A.; Karim, A.; Han, C. C.; Ankner, J. F.; Kaiser, H.; Peiffer, D. G. *Macromolecules* **1996**, *29*, 3918.
(29) Sauer, B. B.; Walsh, D. J. *Macromolecules* **1991**, *24*, 5948.
(30) Composto, R. J.; Kramer, E. J. *J. Mater. Sci.* **1991**, *26*, 2815.
(31) Chiou, J. S.; Barlow, J. W.; Paul, D. R. *J. Polym. Sci., Part B: Polym. Phys.* **1987**, *25*, 1459.
(32) Kim, W. N.; Burns, C. M. *J. Appl. Polym. Sci.* **1990**, *41*, 1575.
(33) Kyu, T.; Lim, D. S. *J. Chem. Phys.* **1990**, *92*, 3951.
(34) Lim, D. S.; Kyu, T. *J. Chem. Phys.* **1990**, *92*, 3944.
(35) Butzbach, G. D.; Wendorff, J. H. *Polymer* **1991**, *32*, 1155.
(36) Nishimoto, M.; Keskkula, H.; Paul, D. R. *Polymer* **1991**, *32*, 272.
(37) Motowoka, M.; Jinnai, H.; Hashimoto, T.; Qiu, Y.; Han, C. C. *J. Chem. Phys.* **1993**, *99*, 2095.
(38) Agari, Y.; Ueda, A.; Omura, Y.; Nagai, S. *Polymer* **1997**, *38*, 801.
(39) Yoon, H.; Feng, Y.; Qiu, Y.; Han, C. C. *J. Polym. Sci., Part B: Polym. Phys.* **1994**, *32*, 1485.
(40) Kienzle, P. A.; O'Donovan, K. V.; Ankner, J. F.; Berk, N. F.; Majkrzak, C. F., http://www.ncnr.nist.gov/reflpak, 2000.
(41) Bucknall, D. G.; Fernandez, M. L.; Higgins, J. S. *Faraday Discuss.* **1994**, *98*, 19.
(42) Fernandez, M. L.; Higgins, J. S.; Penfold, J.; Shackleton, C.; Walsh, D. J. *Polymer* **1990**, *31*, 2146.
(43) Karim, A.; Douglas, J. F.; Satija, S. K.; Han, C. C.; Goyette, R. J. *Macromolecules* **1999**, *32*, 1119.
(44) Lin, E. K.; Wu, W. I.; Satija, S. K. *Macromolecules* **1997**, *30*, 7224.
(45) Karim, A.; Felcher, G. P.; Russell, T. P. *Macromolecules* **1994**, *27*, 6973.
(46) Fernandez, M. L.; Higgins, J. S.; Penfold, J.; Shackleton, C. *J. Chem. Soc., Faraday Trans.* **1991**, *87*, 2055.
(47) Milhaupt, J. M.; Lodge, T. P.; Smith, S. D.; Hamersky, M. W. *Macromolecules* **2001**, *34*, 5561.
(48) Fetters, L. J.; Lohse, D. J.; Colby, R. H. Chain dimensions and entanglement spacings. In *Physical Properties of Polymers Handbook*; Mark, J. E., Ed.; AIP: New York, 1996.
(49) Argon, A. S.; Cohen, R. E.; Patel, A. C. *Polymer* **1999**, *40*, 6991.
(50) Yuan, G.; Li, C.; Satija, S. K.; Karim, A.; Douglas, J. F.; Han, C. C. *Soft Matter* **2010**, *6*, 2153.
(51) Karim, A.; Tsukruk, V. V.; Douglas, J. F.; Satija, S. K.; Fetters, L. J.; Reneker, D. H.; Foster, M. D. *J. Phys. II* **1995**, *5*, 1441.
(52) Douglas, J. F.; Johnson, H. E.; Granick, S. *Science* **1993**, *262*, 2010.
(53) Smith, A. P.; Douglas, J. F.; Amis, E. J.; Karim, A. *Langmuir* **2007**, *23*, 12380.

(54) Certain commercial equipment, instruments, or materials (or suppliers, or software, etc.) are identified in this paper to foster understanding. Such identification does not imply recommendation or endorsement by the National Institute of Standards and Technology, nor does it imply that the materials or equipment identified are necessarily the best available for the purpose.